IOSR Journal of Applied Chemistry (IOSR-JAC)
e-ISSN: 2278-5736.Volume 16, Issue 6 Ser. I (June 2023), PP 27-35
www.iosrjournals.org

Synthesis, Spectroscopic Study, And X-Ray Diffraction Of A New Heptacoordinated Complex Of Mn(II) Derived From (*E*)-4-Methyl-*N*'-((5-Methyl-1*H*-Imidazol-4-Yl)Methylene)Benzohydrazide

Mohamedou El Boukhary[a,c], Thierno Mousa Seck[b], Bocar Traoré[b], FarbaBouyaguiTamboura[a], Ibrahima Elhadj Thiam[b], Aliou Hamady Barry[c], Mohamed Gaye[a*]

[a]*Department of Chemistry, University Alioune Diop, Bambey, Senegal*
[b]*Department of Chemistry, University Cheikh Anta Diop, Dakar, Senegal*
[c]*Unité de Recherche en Chimie des Matériaux, Département de Chimie, Université deNouakchott, Mauritanie*

Abstract
A novel mononuclear manganese(II) complex derived from the ligand (E)-4-methyl-N'-((5-methyl-1H-imidazol-4-yl)methylene)benzohydrazide (H_2L) which was obtained by the condensation reaction between p-toluic hydrazide and 4-methyl-5-imidazolecarboxaldehyde in the presence of glacial acetic acid. The compound was characterized using spectroscopic techniques such as infrared and ^1H and ^{13}C NMR. The mononuclear complex obtained was characterized by spectroscopic FTIR and UV-visible spectroscopy and molar conductivity and magnetic susceptibility measurements at room temperature. The title complex formulated as $[Mn(H_2L)_2Cl_2]$ crystallizes in the triclinic space group P-1 with the following unit cell parameter: a = 9.0482 (3) Å, b = 11.3942 (4) Å, c = 14.6013 (5) Å, α = 68.553 (3)°, β = 81.563 (3)°, γ = 83.744 (3)°, Z = 2, R_1 = 0.076 and wR_2 = 0.211 The asymmetric unit of the crystal structure of the $[Mn(H_2L)_2Cl_2]$ complex is composed of one manganese (II) ion, two molecules of the ligand, and two terminal chloride ions. One of the ligand molecules acts in tridentate fashion through its imino nitrogen atom, its oxygen atom of the carbonyl moiety and one nitrogen atom of the imidazole unit. The second ligand molecule acts in bidentate fashion through its imino nitrogen atom and its oxygen atom of the carbonyl moiety. The coordination polyhedron around the heptacoordinated Mn^{2+} metal center is best described as a distorted pentagonal bipyramid with a $MnN_3O_2Cl_2$ chromophore.

Keywords: *p-Toluic hydrazide; Heptacoordinated ; Manganese ; X-ray diffraction ; Complex ; mononuclear*

Date of Submission: 08-06-2023 Date of Acceptance: 18-06-2023

I. Introduction

In recent years, hydrazone derivatives, especially aroyl-hydrazone have attracted the attention of chemists due to their diverse biological properties and their wide applications in medicinal chemistry [1–3]. The biological activity of these compounds has been attributed to the presence of the (–C(O)NHN=CH–) moiety. Several hydrazone derivatives exhibit a broad spectrum of biological activities such as antibacterial [4–7], antifungal [8–10], anti-inflammatory [11–14], anticonvulsant [15], antioxidant [16–20], antidiabetic [21], antitumor [22–25], antiviral [26, 27], and antidepressant [28–30]. Hydrazone derivatives are widely used as intermediates in the synthesis of heterocyclic compounds [31, 32]. Structurally, hydrazine derivatives exhibit keto-enol tautomerism with the dominant ketone form in the solid state [33]. Theoretically, acylhydrazones can have four isomers, two of which are geometric isomers (*E*/*Z*) due to the C=N double bond, and two are conformational isomers (syn/anti) due to the N–N bond [34–36]. Thus, in a mixture of *E* and *Z* isomers, it has been shown that the *E* isomer is predominant, in general, because its stability is greater than that of the *Z* isomer [37]. In coordination chemistry, the Schiff bases derived from hydrazone are excellent ligands due to their ability to bind metal ions [38–40] and to lead to the formation of supramolecular structures via intermolecular hydrogen bonds [41, 42]. Depending on the reaction conditions, such as the pH, the nature and the oxidation state of the metal ion and the ligand concentration, these Schiff bases coordinate with the metal ions in their neutral amide form, or in their iminolate form [43–45]. The presence of heterocycles presenting a combination

* Corresponding author address : mohamedl.gaye@ucad.edu.sn

of additional donor sites considerably improves the chelating properties of the hydrazone ligands. These Schiff bases have been shown to be useful molecules for building supramolecular structures [45, 46]. In this work we report Mn(II) complex of the aroyl hydrazone ligand formed by condensation of p-toluic hydrazide and 4-methyl-5-imidazolecarboxaldehyde (Scheme 1). X-ray crystal structure of the Mn(II) complex is reported.

II. Experimental part

Materials and method

Manganese(II) chloride tetrahydrate, p-toluic hydrazide, 4-methyl-5-imidazolecarboxaldehyde, and solvent are purchased from Sigma Aldrich. They are used without further treatment. The melting points were recorded on a Büchi apparatus. Infrared spectra were recorded on a Perkin Elmer spectrophometer between 4000–400 cm^{-1}. ^{1}H and ^{13}C NMR spectra of the Schiff base (H_2L) were recorded in DMSO-d_6 on a Bruker 250 MHz spectrometer using TMS as internal reference. UV-Visible spectra were recorded in a DMF solution with a concentration of 10^{-3} M at 25°C on a Perkin Elmer Lambda 365 UV–Visible spectrophotometer. Measurements of the molar conductance of the complex were carried out in a DMF solution with a concentration of 10^{-3} M at 25° C using a WTW LF-330 conductivity meter with a WTW conductivity cell. Room temperature magnetic susceptibilities of the powdered samples were measured using a Johnson Mattey scientific magnetic susceptibility balance (Calibrant: $Hg[Co(SCN)_4]$).

Synthesis of the ligand (*E*)-4-methyl-*N*'-((5-methyl-1*H*-imidazol-4-yl)methylene)benzohydrazide (H_2L)

In a 100 mL flask, (1 g, 6.622 mmol) of p-toluic hydrazide and 20 mL of methanol were mixed and stirred for 30 min under reflux. 4-methyl-5-imidazolecarboxaldehyde (0.6 g, 6.662 mmol), previously dissolved in 10 mL, and few drops of glacial acetic acid were added. The mixture is refluxed for two hours. A clear yellow solution was obtained. After cooling at 4°C, a precipitate appears and collected by filtration, washed with diethyl ether, and dried under vacuum. Yield: 91 %. Tf: > 260°C. IR (ν, cm^{-1}): 3277 (NH); 3153 (NH)imidazole; 1651 (C=O); 1606 $(C=N)_{imine}$; 1568 $(C=N)_{imidazole}$, 1538-1448 (C_{Ar}=C_{Ar}); 1033 (N-N). ^{1}H NMR (DMSO-d_6, δ (ppm)): 2.40 (3H, S, CH_3—Imidazole); 2.50 (3H, S, CH_3—Ar); 7.37 (2H, D, H—Ar); 7.54 (1H, m, $H_{imidazole}$); 7.82 (2H, D, H—Ar); 7.82 (1H, S, H—C=N); 12.71 (1H, m, $NH_{imidazole}$); 14.35 (1H, m, —NH—N=C—). NMR (^{13}C) (DMSO-d_6, δ (ppm)): 161.8 (C=O); 148.33 (C=N), 127.44—135.49 (C_{Ar}) 21.47 (CH_3—Ar); 09.56 (CH_3—Imidazole).

Synthesis of the complex $[Mn(H_2L)_2{\cdot}Cl_2]$

In a 100 mL flask, 20 mL of methanol and H_2L (0.2 g, 0.826 mmol) were added. After stirring at room temperature for a few minutes a white suspension appears. An ethanol solution containing (0.164 g, 0.826 mmol) of manganese chloride tetrahydrate ($MnCl_2{\cdot}4H_2O$) was added. The mixture is kept under stirring for one hour. The resulting colorless solution was filtered and stored for slow evaporation. After two weeks, the white crystals which appeared were recovered. $[Mn(H_2L)_2{\cdot}Cl_2]$. Yield: 76.8 %. Tf > 280. IR (ν, cm^{-1}): 3200 (N—H), 3150 (N—H); 1635 (C=O); 1612 $(C=N)_{imine}$; 1567 $(C=N)_{imidazole}$; 1551 $(C=N)_{imidazole}$; 1534-1447 (C_{Ar}=C_{Ar}); 1044 (N—N). UV-vis (DMF, λ (nm)): 221, 312, 415. Λ (DMF, $\Omega^{-1}{\cdot}cm^2{\cdot}mol^{-1}$): fresh solution: 6.7; after fifteen days: 10.1. μ_{eff}: 5.35 μ_B.

X-ray data collection structure determination and refinement

Single crystals of $[Mn(H_2L)_2{\cdot}Cl_2]$ were grown by slow evaporation of MeOH solution of the complex. A suitable crystal was selected and mounted on a Kappa single XtaLAB AFC12 (RINC): Kappa single diffractometer Radiation source: micro-focus sealed X-ray tube Rigaku (Mo)mm03 X-ray Source with graphite monochromatized MoKα radiation (λ = 0.710173). Data were collected at the temperature of 293 K. Details of the X-ray crystal structure solution and refinement are given in Table 1. The structure was solved with the SHELXT [47] structure solution program using direct methods and refined with the SHELXTL [48] software package. The hydrogen atoms of water molecules and NH groups were located in the Fourier difference maps and refined. Molecular graphics were generated using ORTEP [49].

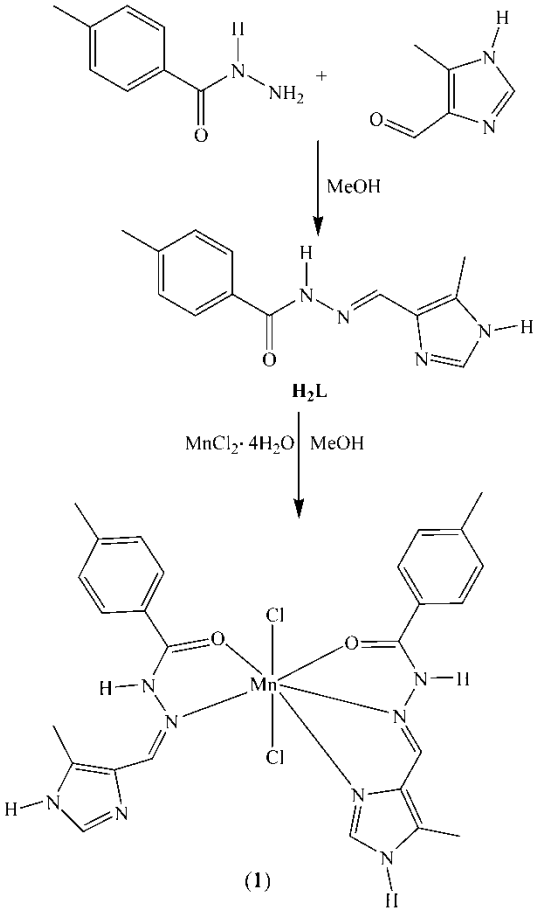

Scheme 1. Synthesis procedure of the complex $[Mn(H_2L)_2Cl_2]$.

Table-1. Crystallographic data and refinement parameter for the Mn(II) complex.

Chemical formula	$C_{26}H_{28}Cl_2MnN_8O_2$ (**1**)
*M*r (g/mol)	610.40
Crystal system	Triclinic
Space group	Pī
Temperature (K)	100
a (Å)	9.0482 (3)
b (Å)	11.3942 (4)
c (Å)	14.6013 (5)
α (°)	68.553 (3)
β (°)	81.563 (3)
γ (°)	83.744 (3)
V (Å^3)	1383.45 (9)
Z	2
D_x (g/cm^3)	1.465
μ (mm^{-1})	0.71
F(000)	630
Crystal size (mm^3)	0.1 × 0.04 × 0.03
Mo *K*α (Å)	0.71073
θ range (°)	2.4–74.8
h k l ranges	$-15 \le h \le 15$; $-19 \le k \le 19$; $-24 \le l \le 24$
T_{min}, T_{max}	0.857, 0.950
No. of measured reflections	34889
No. of independent reflections	11466
No. of observed [$I > 2\sigma(I)$] reflections	4568
R_{int}	0.136
$R[F^2 > 2\sigma(F^2)]$	0.076
$wR(F^2)$	0.211
Goodness-of-fit on F^2	0.96
Data/restraints/parameters	11466/0/356
$\Delta\rho_{max}$, $\Delta\rho_{min}$ (eÅ^{-3})	1.40, −0.71

Table-2. Selected interatomic distances (Å) and bond angle (°) for the Mn(II) complex.

Mn1—Cl2	2.6100 (9)	Cl1—Mn1—Cl2	178.83 (3)
Mn1—Cl1	2.5247 (9)	N6—Mn1—O2	66.79 (9)
Mn1—O1	2.243 (2)	N7—Mn1—N6	69.32 (9)
Mn1—O2	2.365 (2)	O1—Mn1—Cl1	93.48 (7)
Mn1—N6	2.318 (3)	O1—Mn1—N2	69.55 (9)
Mn1—N2	2.378 (3)	O1—Mn1—N7	75.14 (9)
Mn1—N7	2.307 (3)	O2—Mn1—N2	79.11 (9)
O1—C8	1.236 (4)	N2—Mn1—Cl2	88.60 (7)
O2—C21	1.241 (4)	N2—Mn1—Cl1	91.02 (7)
N6—N5	1.366 (4)	N7—Mn1—Cl1	92.53 (7)

III. Results and discussion

General studies

The ^{1}H and ^{13}C NMR spectra of the H_2L ligand were recorded in DMSO-d_6. On the ^{1}H NMR spectrum, signals at 12.71 ppm and 14.35 ppm are respectively assigned to the N—H proton of the imidazole group and N—H proton of the hydrazone moiety [6]. The H—Ar protons of the phenyl and the imidazole rings are pointed in the range 7.37—7.82 ppm. The characteristic signal of the imine proton appears at 7.98 ppm [50]. The signals of the two methyl groups linked to the imidazole and the phenyl rings are pointed at 2.40 ppm and 2.5 ppm, respectively. The ^{13}C NMR spectrum reveals two characteristic signals at 161.8 ppm and 148.33 ppm of the carbon atoms of the C=O and C=N moieties [6]. The signals due to the carbon atoms of the aromatic rings are pointed in the range [127.52-135.49] ppm. The signals of the carbon atoms of the two methyl groups are identified, respectively, at 21.47 ppm (CH_3—Ar) and 9.56 ppm (CH_3—imidazole). The FTIR spectrum of the ligand shows vibration bands at 1651 cm^{-1}, 1606 cm^{-1} and 1568 cm^{-1} attributed, respectively, to $\nu_{C=O}$ and $\nu_{C=N}$ of the imine and the imidazole moieties [41, 51, 52]. These bands are shifted upon complexation of the ligand with the manganese(II) ion. They are pointed, respectively, at 1635 cm^{-1}, 1612 cm^{-1} and 1551 cm^{-1}. These facts are indicative of the involvement of the carbonyl oxygen atoms, the imine nitrogen atoms, and the imidazole nitrogen atom in the coordination of the ligand to the manganese atom. The molar conductance of the 10^{-3} M solution of the metal complex in DMF was measured at 25°C. The values of the molar conductivity of the fresh solution of the metal complex and fifteen days later are respectively 6.7 $\Omega^{-1}\cdot cm^2\cdot mol^{-1}$ and 10.1 $\Omega^{-1}\cdot cm^2\cdot mol^{-1}$. These values indicate a neutral electrolyte nature ang good stability of the complex in DMF [53]. The UV-visible spectrum of the complex was recorded in DMF. The spectrum shows bands at 221 nm, 312 nm, and 415 nm. They are, respectively, characteristic of the $\pi\rightarrow\pi^*$, $n\rightarrow\pi^*$ transition intra-ligand bands [54] and the electronic charge transfer from the ligand to the metal (TCLM) [55, 56]. The value of the magnetic moment taken at the ambient temperature of the complex is 5.35 μ_B. This value is close proximity to those of the mononuclear heptacoordinated complexes $[Mn(H_2L)_2(H_2O)_2]\cdot(ClO_4)_2\cdot 3(H_2O)$ (H_2L: *N,N*'-1,5-bis (pyridylmethylidene)carbonohydrazone (5.25 BM) [57] and $Mn(H_2L)(H_2O)Cl_2]$ (H_2L: *N,N*'-1,5-bis(2-acetylpyridinyl)-carbonohydrazone (5.33 BM) [55].

Description of the crystal structure

The complex crystallizes in the triclinic system with the space group P-1. Selected bond angles and interatomic distances are listed in Table 2. The crystal structure of the complex with the chemical formula $[Mn(H_2L)_2Cl_2]$ is shown in Figure 1. The asymmetric unit of the complex is composed of one Mn(II) ion, two molecules of the ligand and two chloride anions. One of the molecules of the ligand acts in tridentate fashion through a carbonyl oxygen atom, an azomethine nitrogen atom and a nitrogen atom of the imidazole ring. The other organic molecule acts as a bidentate ligand through a carbonyl oxygen atom and an azomethine nitrogen atom. The bidentate ligand forms one five membered ring of type MnOCNN with bite angle of 69.55 (9)° [O1—Mn1—N2]. The three dentate ligand form two five membered ring of types MnOCNN and MnNCCN with bite angle values of 66.79 (9)° [O2—Mn1—N6] and 69.32 (9)° [n6—Mn1—N7]. The geometry around the Mn(II) ion is described as a distorted pentagonal base bipyramid with a $MnN_3O_2Cl_2$ Chromophore. The basal plane is formed by two azomethine nitrogen atoms, two carbonyl oxygen atoms coming from two different organic molecules, and one imidazole nitrogen atom of one of two different ligand molecules. The axial positions are occupied by the two chloride ions. Thus, the manganese (II) ion is heptacoordinated (Figure 1). The angles formed between the manganese (II) ion and the atoms occupying the basal plane are in the range [79.11 (9)°—66.79 (9)°. These angle values are deviated from the ideal angle value [72°] expected for a regular pentagon geometry. The atoms situated in the basal plane and the Mn(II) ion are quite coplanar (rms = 0.0449) with a

maximum deviation observed for one of the carbonyl oxygen atom (O2) which is out of the plane by 0.0664(2) Å. The sum of angles subtended by the atoms in the basal plane is 359.91°. The value of the angle subtended by the terminal chloride atoms occupying the apical positions is 178.83 (3)° [Cl1-Mn1-Cl2] and deviate slightly of ideal value of 180° expected for a regular pentagonal bipyramid. The five membered ring Mn1/O1/C8/N1/N2 of the bidentate ligand and the five membered ring of the tridentate ligand Mn1/N7/C23/C22/N6 are quite coplanar with the dihedral angle of 1.698(2)°. The two five membered rings of type Mn1/O1/C8/N1/N2 and Mn1/O2/C21/N5/N6 defined by the two different molecules ligand upon coordination, are slightly twisted with a dihedral angle value of 3.780(2)°. The two five membered rings Mn1/O2/C21/N5/N6 and Mn1/N7/C23/C22/N6 defined upon coordination of the tridentate ligand molecule are slightly twisted with a dihedral angle value of 4.881(2)°. The lengths of the bonds in equatorial plane : Mn1—O1 = 2.243 (2) Å, Mn1—O2 = 2.365 (2) Å, Mn1—N7 = 2.307 (3) Å, Mn1—N2 = 2.378 (3) Å, Mn1—N6 = 2.318 (3) Å are shorted than the bonds length values defined by the atoms in the apical positions : Mn1—Cl1= 2.5247 (9) Å and Mn1—Cl2 = 2.6100 (9) Å. The Mn—O, and Mn—N distances are close to those observed within manganese (II) complexes [57–59], while the Mn—Cl distances are comparable to those reported for the similar complex $[Mn(L)(Cl)_2]\cdot(MeOH)$ [58] (*L* is 2,6-bis[(2-hydroxyphenylimino)methyl]pyridine).The hydrogen bonding geometry of the compound is listed in Table 3. Intramolecular hydrogen bond N1—H1⋯N3 resulting in a *S*(6) ring and weak hydrogen bond C9—H9⋯O2 have been observed. In the crystal the molecules of the complex are linked by hydrogen bonds giving rise to a three-dimensional network (Figure 2, Table 3).The structure is built up from pentagonal bipyramids around the Mn^{2+} ion which are assembled in layers parallel to the *bc* plane. The layers are interconnected by intermolecular hydrogen-bonds. The axial chloride atoms point in the interlayer space and act as hydrogen-bond acceptors toward N8—H8⋯Cl2^{i},N5—H5⋯Cl2^{ii},N4—H4⋯Cl2^{iii},C22—H22⋯Cl1^{ii}, [symmetry codes : (i) −x+1, −y, −z+1; (ii) −x+1, −y+1, −z+1; (iii) −x+2, −y+1, −z]. The crystal packing of the compound is stabilized by weak intermolecular hydrogen bonds of type C–H⋯N(hydrazinyl) (C13—H13A⋯N1^{iii}, iii = −x+2, −y+1, −z) and C—H⋯Cl (C22—H22⋯Cl1^{ii}, ii = −x+1, −y+1, −z+1; C11—H11⋯Cl1^{iv}, iv = −x+1, −y+1, −z) (Figure 2, Table 3).

Table-3. Hydrogen-bond geometry (Å, °) for the Mn(II) complex.

D—H⋯*A*	*D*—H	H⋯*A*	*D*⋯*A*	*D*—H⋯*A*
N1—H1⋯N3	0.88	1.91	2.618 (4)	136.8
N8—H8⋯Cl2^{i}	0.88	2.32	3.163 (3)	159.3
N5—H5⋯Cl1^{ii}	0.88	2.47	3.286 (3)	154.6
N4—H4⋯Cl2^{iii}	0.88	2.26	3.121 (3)	167.3
C22—H22⋯Cl1^{ii}	0.95	2.76	3.545 (3)	140.4
C9—H9⋯O2	0.95	2.51	3.122 (4)	122.5
C13—H13A⋯N1^{iii}	0.98	2.66	3.573 (4)	155.4
C11—H11⋯Cl1^{iv}	0.95	2.97	3.753 (4)	140.7

Symmetry codes: (i) −x+1, −y, −z+1; (ii) −x+1, −y+1, −z+1; (iii) −x+2, −y+1, −z; (iv) −x+1, −y+1, −z.

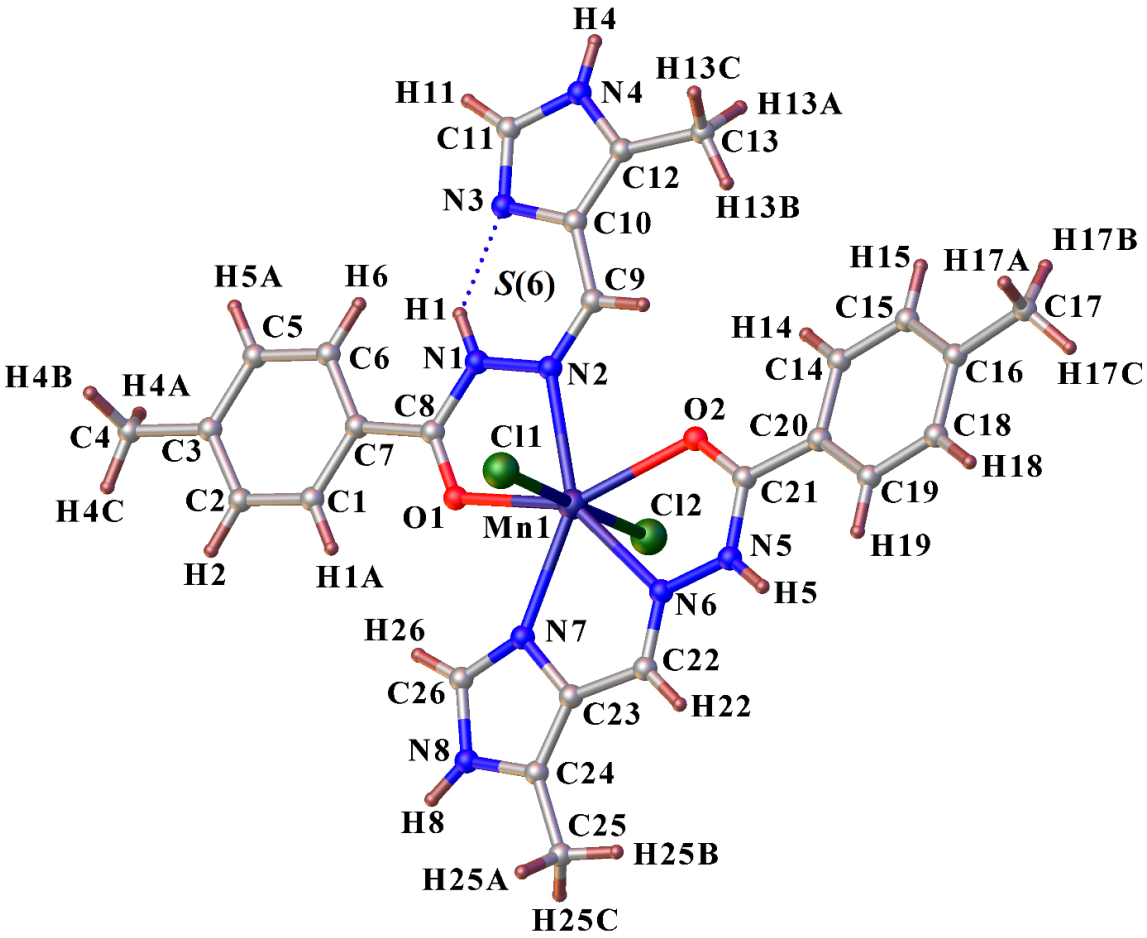

Figure 1. Crystal structure of the complex $[Mn(H_2L)_2Cl_2]$.

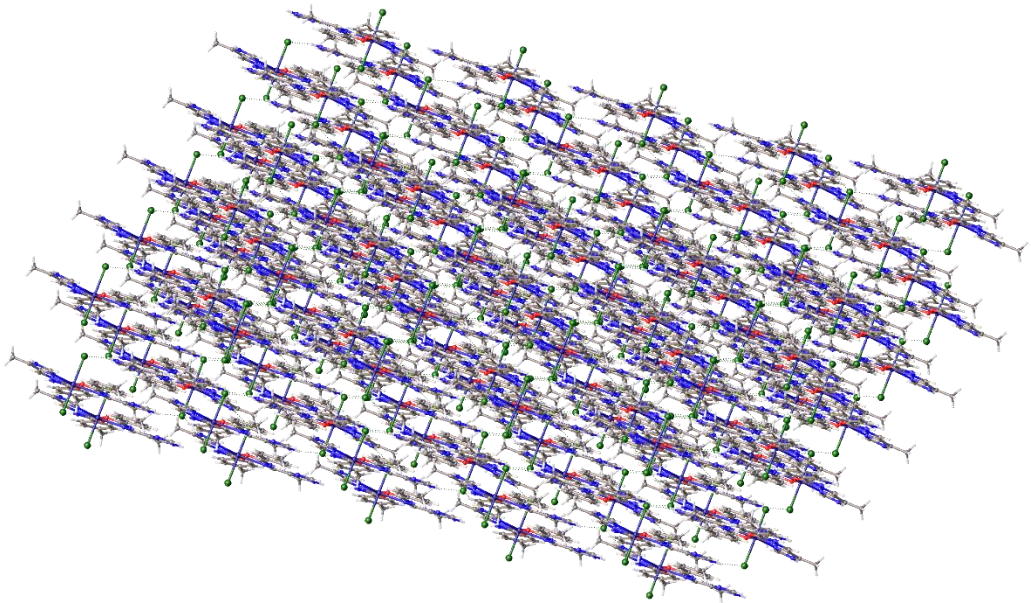

Figure 2.Three-dimensional structure of the complex $[Mn(H_2L)_2Cl_2]$.

IV. Conclusion

The mononuclear complex $[Mn(H_2L)_2Cl_2]$ was synthesized from (*E*)-4-methyl-*N*'-((5-methyl-1*H*-imidazol-4-yl)methylene)benzohydrazide (H_2L) and manganese chloride tetrahydrate in an alcoholic medium. Spectroscopic techniques such as infrared, UV-visible and measurements of molar conductivity and magnetic susceptibility at room temperature were used for the characterization of the complex. The values of the molar

conductivity of the fresh solution and fifteen days after showed a neutral electrolyte behavior and a high stability of the complex in the DMF. The value of the magnetic moment at room temperature of the complex agrees with a mononuclear manganese complex of high spin d^5 configuration. X-ray diffraction analysis confirmed the conductimetric and magnetic data at temperature. It reveals a neutral mononuclear complex. The Mn^{2+} ion is situated in a distorted pentagonal bipyramid environment defined by $N_3O_2Cl_2$ inner. Intramolecular and intermolecular hydrogen bonds consolidate the structure.

Supplementary Materials

CCDC-2267668 contains the supplementary crystallographic data for this paper. These data can be obtained free of charge via https://www.ccdc.cam.ac.uk/structures/or by e-mailing data_request@ccdc.cam.ac.uk or by contacting The Cambridge Crystallographic Data Centre 12 Union Road Cambridge CB2 1EZ UK; fax: +44(0)1223-336033.

Reference :

[1]. Socea, L.-I., Barbuceanu, S.-F., Pahontu, E. M., Dumitru, A.-C., Nitulescu, G. M., Sfetea, R. C., Apostol, T.-V. (2022). Acylhydrazones and Their Biological Activity: A Review. Molecules, 27(24), 8719. https://doi.org/10.3390/molecules27248719

[2]. Xia, L., Xia, Y.-F., Huang, L.-R., Xiao, X., Lou, H.-Y., Liu, T.-J., Pan, W.-D., Luo, H. (2015). Benzaldehyde Schiff bases regulation to the metabolism, hemolysis, and virulence genes expression in vitro and their structure–microbicidal activity relationship. European Journal of Medicinal Chemistry, 97, 83–93. https://doi.org/10.1016/j.ejmech.2015.04.042

[3]. Mali, S. N., Thorat, B. R., Gupta, D. R., Pandey, A. (2021). Mini-Review of the Importance of Hydrazides and Their Derivatives—Synthesis and Biological Activity. Engineering Proceedings, 11(1), 21. https://doi.org/10.3390/ASEC2021-11157

[4]. Morjan, R. Y., Mkadmh, A. M., Beadham, I., Elmanama, A. A., Mattar, M. R., Raftery, J., Pritchard, R. G., Awadallah, A. M., Gardiner, J. M. (2014). Antibacterial activities of novel nicotinic acid hydrazides and their conversion into N-acetyl-1,3,4-oxadiazoles. Bioorganic Medicinal Chemistry Letters, 24(24), 5796–5800. https://doi.org/10.1016/j.bmcl.2014.10.029

[5]. Zhou, Y., Zhang, S., He, H., Jiang, W., Hou, L., Xie, D., Cai, M., Peng, H., Feng, L. (2018). Design and synthesis of highly selective pyruvate dehydrogenase complex E1 inhibitors as bactericides. Bioorganic Medicinal Chemistry, 26(1), 84–95. https://doi.org/10.1016/j.bmc.2017.11.021

[6]. Rezki, N., Al-Sodies, S. A., Ahmed, H. E. A., Ihmaid, S., Messali, M., Ahmed, S., Aouad, M. R. (2019). A novel dicationic ionic liquids encompassing pyridinium hydrazone-phenoxy conjugates as antimicrobial agents targeting diverse high resistant microbial strains. Journal of Molecular Liquids, 284, 431–444. https://doi.org/10.1016/j.molliq.2019.04.010

[7]. Rohane, S. H., Chauhan, A. J., Fuloria, N. K., Fuloria, S. (2020). Synthesis and in vitro antimycobacterial potential of novel hydrazones of eugenol. Arabian Journal of Chemistry, 13(2), 4495–4504. https://doi.org/10.1016/j.arabjc.2019.09.004

[8]. Siddique, M., Saeed, A. B., Dogar, N. A., Ahmad, S. (2013). Biological Potential of Synthetic Hydrazide Based Schiff Bases. Journal of Scientific Innovative Research, 2(3), 651–657.

[9]. Guilherme, F. D., Simonetti, J. É., Folquitto, L. R. S., Reis, A. C. C., Oliver, J. C., Dias, A. L. T., Dias, D. F., Carvalho, D. T., Brandão, G. C., Souza, T. B. de. (2019). Synthesis, chemical characterization, and antimicrobial activity of new acylhydrazones derived from carbohydrates. Journal of Molecular Structure, 1184, 349–356. https://doi.org/10.1016/j.molstruc.2019.02.045

[10]. Reis, D. C., Despaigne, A. A. R., Silva, J. G. D., Silva, N. F., Vilela, C. F., Mendes, I. C., Takahashi, J. A., Beraldo, H. (2013). Structural Studies and Investigation on the Activity of Imidazole-Derived Thiosemicarbazones and Hydrazones against Crop-Related Fungi. Molecules, 18(10), 12645–12662. https://doi.org/10.3390/molecules181012645

[11]. Avila, C. M., Lopes, A. B., Gonçalves, A. S., Silva, L. L. da, Romeiro, N. C., Miranda, A. L. P., Sant'Anna, C. M. R., Barreiro, E. J., Fraga, C. A. M. (2011). Structure-based design and biological profile of (E)-N-(4-Nitrobenzylidene)-2-naphthohydrazide, a novel small molecule inhibitor of IκB kinase-β. European Journal of Medicinal Chemistry, 46(4), 1245–1253. https://doi.org/10.1016/j.ejmech.2011.01.045

[12]. Cerqueira, J. V., Meira, C. S., Santos, E. de S., França, L. S. de A., Vasconcelos, J. F., Nonaka, C. K. V., de Melo, T. L., Filho, J. M. dos S., Moreira, D. R. M., Soares, M. B. P. (2019). Anti-inflammatory activity of SintMed65, an N-acylhydrazone derivative, in a mouse model of allergic airway inflammation. International Immunopharmacology, 75, 105735. https://doi.org/10.1016/j.intimp.2019.105735

[13]. Meira, C. S., Filho, J. M. dos S., Sousa, C. C., Anjos, P. S., Cerqueira, J. V., Neto, H. A. D., da Silveira, R. G., Russo, M. R., Wolfender, J.-L., Queiroz, E. F., Moreira, D. R. M., Soares, M. B. P. (2018). Structural design, synthesis, and substituent effect of hydrazone-N-acylhydrazones reveal potent immunomodulatory agents. Bioorganic Medicinal Chemistry, 26(8), 1971–1985. https://doi.org/10.1016/j.bmc.2018.02.047

[14]. Moraes, A. D. T. de O., Miranda, M. D. S. de, Jacob, Í. T. T., Amorim, C. A. da C., Moura, R. O. de, Silva, S. Â. S. da, Soares, M. B. P., de Almeida, S. M. V., Souza, T. R. C. de L., Lima, de Oliveira, J. F., de Silva, T. G., de Melo, C. M. L., Moreira, D. R. M., de Lima, M. do C. A. (2018). Synthesis, in vitro and in vivo biological evaluation, COX-1/2 inhibition, and molecular docking study of indole-N-acylhydrazone derivatives. Bioorganic Medicinal Chemistry, 26(20), 5388–5396. https://doi.org/10.1016/j.bmc.2018.07.024

[15]. Shakdofa, M. M. E., Shtaiwi, M. H., Morsy, N., Abdel-rassel, T. M. A. (2014). Metal complexes of hydrazones and their biological, analytical, and catalytic applications: A review. Main Group Chemistry, 13(3), 187–218. https://doi.org/10.3233/MGC-140133

[16]. Duarte, C. D., Tributino, J. L. M., Lacerda, D. I., Martins, M. V., Alexandre-Moreira, M. S., Dutra, F., Bechara, E. J. H., de Paula, F. S., Goulart, M. O. F., Ferreira, J., Calixto, J. B., Nunes, M. P., Bertho, A. L., Miranda, A. L. P., Barreiro, E. J., Fraga, C. A. M. (2007). Synthesis, pharmacological evaluation, and electrochemical studies of novel 6-nitro-3,4-methylenedioxyphenyl-N-

acylhydrazone derivatives: Discovery of LASSBio-881, a new ligand of cannabinoid receptors. Bioorganic Medicinal Chemistry, 15(6), 2421–2433.
https://doi.org/10.1016/j.bmc.2007.01.013

[17]. Tributino, J. L. M., Duarte, C. D., Corrêa, R. S., Doriguetto, A. C., Ellena, J., Romeiro, N. C., Castro, N. G., Miranda, A. L., P., Barreiro, E. J, Fraga, C. A. M. (2009). Novel 6-methanesulfonamide-3,4-methylenedioxyphenyl-N-acylhydrazones: Orally effective anti-inflammatory drug candidates. Bioorganic Medicinal Chemistry, 17(3), 1125–1131. https://doi.org/10.1016/j.bmc.2008.12.045

[18]. Demurtas, M., Baldisserotto, A., Lampronti, I., Moi, D., Balboni, G., Pacifico, S., Vertuani, S., Manfredini, S., Onnis, V. (2019). Indole derivatives as multifunctional drugs: Synthesis and evaluation of antioxidant, photoprotective and antiproliferative activity of indole hydrazones. Bioorganic Chemistry, 85, 568–576. https://doi.org/10.1016/j.bioorg.2019.02.007

[19]. Anastassova, N. O., Yancheva, D. Y., Mavrova, A. T., Kondeva-Burdina, M. S., Tzankova, V. I., Hristova-Avakumova, N. G., Hadjimitova, V. A. (2018). Design, synthesis, antioxidant properties and mechanism of action of new N,N′-disubstituted benzimidazole-2-thione hydrazone derivatives. Journal of Molecular Structure, 1165, 162–176.
https://doi.org/10.1016/j.molstruc.2018.03.119

[20]. Socea, L. I., Visan, D. C., Barbuceanu, S. F., Apostol, T. V., Bratu, O. G., Socea, B. (2018). The Antioxidant Activity of Some Acylhydrazones with Dibenzo[a,d][7]annulene Moiety. Revista de Chimie, 69(4), 795–797.
https://doi.org/10.37358/RC.18.4.6202

[21]. Tariq, Q.-N., Malik, S., Khan, A., Naseer, M. M., Khan, S. U., Ashraf, A., Rafiq, M., Mahmood, K., Tahir, M. N., Shafiq, Z. (2019). Xanthenone-based hydrazones as potent α-glucosidase inhibitors: Synthesis, solid state self-assembly and in silico studies. Bioorganic Chemistry, 84, 372–383.
https://doi.org/10.1016/j.bioorg.2018.11.053

[22]. Aneja, B., Khan, N. S., Khan, P., Queen, A., Hussain, A., Rehman, M. T., Alajmi, M. F., El-Seedi, H. R., Ali, S., Hassan M. I., Abid, M. (2019). Design and development of Isatin-triazole hydrazones as potential inhibitors of microtubule affinity-regulating kinase 4 for the therapeutic management of cell proliferation and metastasis. European Journal of Medicinal Chemistry, 163, 840–852. https://doi.org/10.1016/j.ejmech.2018.12.026

[23]. Salum, L. B., Mascarello, A., Canevarolo, R. R., Altei, W. F., Laranjeira, A. B. A., Neuenfeldt, P. D., Stumpf, T. R., Chiaradia-Delatorre, L. D., Vollmer, L. L., Daghestani, H. N., Melo, C. P. de S., Silveira, A. B., Leal, P. C., Frederico, M. J. S., do Nascimento, L. F., Santos, A. R. S., Andricopulo, A. D., Day, B. W., Yunes, R. A., Vogt, A., Yunes, J. A., Nunes, R. J. (2015). N-(1′-naphthyl)-3,4,5-trimethoxybenzohydrazide as microtubule destabilizer: Synthesis, cytotoxicity, inhibition of cell migration and in vivo activity against acute lymphoblastic leukemia. European Journal of Medicinal Chemistry, 96, 504–518.
https://doi.org/10.1016/j.ejmech.2015.02.041

[24]. Govindaiah, P., Dumala, N., Mattan, I., Grover, P., Prakash, M. J. (2019). Design, synthesis, biological and in silico evaluation of coumarin-hydrazone derivatives as tubulin targeted antiproliferative agents. Bioorganic Chemistry, 91, 103143.
https://doi.org/10.1016/j.bioorg.2019.103143
Sreenivasulu, R., Reddy, K. T., Sujitha, P., Kumar, C. G., Raju, R. R. (2019). Synthesis, antiproliferative and apoptosis induction potential activities of novel bis(indolyl)hydrazide-hydrazone derivatives. Bioorganic Medicinal Chemistry, 27(6), 1043–1055. https://doi.org/10.1016/j.bmc.2019.02.002

[25]. Tian, B., He, M., Tang, S., Hewlett, I., Tan, Z., Li, J., Tin, Y., Yang, M. (2009). Synthesis and antiviral activities of novel acylhydrazone derivatives targeting HIV-1 capsid protein. Bioorganic Medicinal Chemistry Letters, 19(8), 2162–2167.
https://doi.org/10.1016/j.bmcl.2009.02.116

[26]. Yoneda, J. D., Albuquerque, M. G., Leal, K. Z., Santos, F. da C., Batalha, P. N., Brozeguini, L., Seidl, P. R., de Alencastro, R. B., Cunha, A. C., de Souza, M. C. B. V., Ferreira, V. F., Giongo, V., Cirne-Santos, A., Paixão, I. C. P. (2014). Docking of anti-HIV-1 oxoquinoline-acylhydrazone derivatives as potential HSV-1 DNA polymerase inhibitors. Journal of Molecular Structure, 1074, 263–270.
https://doi.org/10.1016/j.molstruc.2014.05.081

[27]. Cruz-Navarro, A., Hernández-Romero, D., Flores-Parra, A., Rivera, J. M., Castillo-Blum, S. E., Colorado-Peralta, R. (2021). Structural diversity and luminescent properties of coordination complexes obtained from trivalent lanthanide ions with the ligands: tris((1H-benzo[d]imidazol-2-yl)methyl)amine and 2,6-bis(1H-benzo[d]imidazol-2-yl)pyridine. Coordination Chemistry Reviews, 427, 213587.
https://doi.org/10.1016/j.ccr.2020.213587

[28]. 29. Serafim, R. A. M., Gonçalves, J. E., Souza, F. P. de, Loureiro, A. P. de M., Storpirtis, S., Krogh, R., Andricopulo; A. D., Dias, L. C., Ferreira, E. I. (2014). Design, synthesis and biological evaluation of hybrid bioisoster derivatives of N-acylhydrazone and furoxan groups with potential and selective anti-Trypanosoma cruzi activity. European Journal of Medicinal Chemistry, 82, 418–425. https://doi.org/10.1016/j.ejmech.2014.05.077

[29]. 30. Inam, A., Siddiqui, S. M., Macedo, T. S., Moreira, D. R. M., Leite, A. C. L., Soares, M. B. P., Azam, A. (2014). Design, synthesis and biological evaluation of 3-[4-(7-chloro-quinolin-4-yl)-piperazin-1-yl]-propionic acid hydrazones as antiprotozoal agents. European Journal of Medicinal Chemistry, 75, 67–76.
https://doi.org/10.1016/j.ejmech.2014.01.023

[30]. Başpınar Küçük, H., Alhonaish, A., Yıldız, T., Güzel, M. (2022). An efficient approach to access 2,5-disubstituted 1,3,4-oxadiazoles by oxidation of 2-arenoxybenzaldehyde N-acyl hydrazones with molecular iodine. ChemistrySelect, 7(26), e202201391. https://doi.org/10.1002/slct.202201391

[31]. Pelipko, V. V., Gomonov, K. A. (2021). Formation of five- and six-membered nitrogen-containing heterocycles on the basis of hydrazones derived from α-dicarbonyl compounds (microreview). Chemistry of Heterocyclic Compounds, 57(6), 624–626. https://doi.org/10.1007/s10593-021-02958-8

[32]. Jamadar, A., Duhme-Klair, A.-K., Vemuri, K., Sritharan, M., Dandawate, P., Padhye, S. (2012). Synthesis, characterisation and antitubercular activities of a series of pyruvate-containing aroylhydrazones and their Cu-complexes. Dalton Transactions, 41(30), 9192–9201. https://doi.org/10.1039/C2DT30322A

[33]. Purandara, H., Raghavendra, S., Foro, S., Patil, P., Gowda, B. T., Dharmaprakash, S. M., Vishwanatha, P. (2019). Synthesis, spectroscopic characterization, crystal structure, Hirshfeld surface analysis and third-order nonlinear optical properties of 2-(4-chlorophenoxy)-N'-[(1E)-1-(4-methylphenyl) ethylidene] acetohydrazide. Journal of Molecular Structure, 1185, 205–211. https://doi.org/10.1016/j.molstruc.2019.02.079

[34]. Polo-Cerón, D., Hincapié-Otero, M. M., Joaqui-Joaqui, A. (2021). Synthesis and characterization of four N-acylhydrazones as potential O,N,O donors for Cu^{2+}: An experimental and theoretical study. Universitas Scientiarum, 26(2), 193–215. https://doi.org/10.11144/Javeriana.SC26-2.saco

[35]. Ţînţaş, M. L., Diac, A. P., Soran, A., Terec, A., Grosu, I., Bogdan, E. (2014). Structural characterization of new 2-aryl-5-phenyl-1,3,4-oxadiazin-6-ones and their N-aroylhydrazone precursors. Journal of Molecular Structure, 1058, 106–113. https://doi.org/10.1016/j.molstruc.2013.11.005

[36]. Gamov, G. A., Khodov, I. A., Belov, K. V., Zavalishin, M. N., Kiselev, A. N., Usacheva, T. R., Sharnin, V. A. (2019). Spatial structure, thermodynamics, and kinetics of formation of hydrazones derived from pyridoxal 5′-phosphate and 2-furoic, thiophene-2-carboxylic hydrazides in solution. Journal of Molecular Liquids, 283, 825–833. https://doi.org/10.1016/j.molliq.2019.03.125

[37]. Dasgupta, S., Karim, S., Banerjee, S., Saha, M., Das Saha, K., Das, D. (2020). Designing of novel zinc(ii) Schiff base complexes having acyl hydrazone linkage: study of phosphatase and anti-cancer activities. Dalton Transactions, 49(4), 1232–1240. https://doi.org/10.1039/C9DT04636D

[38]. Chen, X.-Q., Cai, Y.-D., Jiang, W., Peng, G., Fang, J.-K., Liu, J.-L., Tong, M.-L., Bao, X. (2019). A Multi-Stimuli-Responsive Fe(II) SCO Complex Based on an Acylhydrazone Ligand. Inorganic Chemistry, 58(2), 999–1002. https://doi.org/10.1021/acs.inorgchem.8b02922

[39]. Faye, M., Gueye, M. N., Dieng, M., Tamboura, F. B., Gaye, M. (2023). Crystal structure of Y(III) Complex with the Tridentate Schiff Base Ligand N'–(1–(pyridin–2–yl)ethylidene)nicotinohydrazide. International Journal of Novel Research in Physics Chemistry Mathematics, 10(1), 60-66.

[40]. https://doi.org/10.5281/zenodo.7876199

[41]. Kuriakose, D., Kurup, M. R. P. (2019). Crystal structures and supramolecular architectures of ONO donor hydrazone and solvent exchangeable dioxidomolybdenum(VI) complexes derived from 3,5-diiodosalicyaldehyde-4-methoxybenzoylhydrazone: Hirshfeld surface analysis and interaction energy calculations. Polyhedron, 170, 749–761. https://doi.org/10.1016/j.poly.2019.06.041

[42]. Yang, H.-L., Dang, Z.-J., Zhang, Y.-M., Wei, T.-B., Yao, H., Zhu, W., Fan, Y.-Q., Jiang, X.-M., Lin, Q. (2019). Novel cyanide supramolecular fluorescent chemosensor constructed from a quinoline hydrazone functionalized-pillar[5]arene. Spectrochimica Acta Part A: Molecular and Biomolecular Spectroscopy, 220, 117136. https://doi.org/10.1016/j.saa.2019.117136

[43]. Galić, N., Rubčić, M., Magdić, K., Cindrić, M., Tomišić, V. (2011). Solution and solid-state studies of complexation of transition-metal cations and Al(III) by aroylhydrazones derived from nicotinic acid hydrazide. Inorganica Chimica Acta, 366(1), 98–104. https://doi.org/10.1016/j.ica.2010.10.017

[44]. Mishra, D., Naskar, S., Blake, A. J., Chattopadhyay, S. K. (2007). Synthesis, characterization, spectroscopic and electrochemical properties of trans,trans,trans-bis(triphenyl phosphine) bis(aroyl hydrazonato)ruthenium(II) complexes. Inorganica Chimica Acta, 360(7), 2291–2297. https://doi.org/10.1016/j.ica.2006.11.012

[45]. Naskar, S., Naskar, S., Mondal, S., Majhi, P. K., Drew, M. G. B., Chattopadhyay, S. K. (2011). Synthesis and spectroscopic properties of cobalt(III) complexes of some aroyl hydrazones: X-ray crystal structures of one cobalt(III) complex and two aroyl hydrazone ligands. Inorganica Chimica Acta, 371(1), 100–106. https://doi.org/10.1016/j.ica.2011.03.051

[46]. Mondal, S., Naskar, S., Dey, A. K., Sinn, E., Eribal, C., Herron, S. R., Chattopadhyay, S. K. (2013). Mononuclear and binuclear Cu(II) complexes of some tridentate aroyl hydrazones. X-ray crystal structures of a mononuclear and a binuclear complex. Inorganica Chimica Acta, 398, 98–105. https://doi.org/10.1016/j.ica.2012.12.018

[47]. Sheldrick G. M. Integrated space-group and crystal-structure determination. Acta Crystallographica Section A. 2015, 71, 3–8. https://doi.org/10.1107/S2053273314026370

[48]. Sheldrick G. M. Crystal structure refinement with SHELXL. Acta Crystallographica Section C. 2015, 71, 3–8. https://doi.org/10.1107/S2053229614024218

[49]. Farrugia, L. J. (2012). WinGX and ORTEP for Windows: an update. Journal of Applied Crystallography, 45(4), 849–854. https://doi.org/10.1107/S0021889812029111

[50]. Zhou, Y., Zhang, S., He, H., Jiang, W., Hou, L., Xie, D., Cai, M., Peng, H., Feng, L. (2018). Design and synthesis of highly selective pyruvate dehydrogenase complex E1 inhibitors as bactericides. Bioorganic Medicinal Chemistry, 26(1), 84–95. https://doi.org/10.1016/j.bmc.2017.11.021

[51]. Sadhukhan, D., Maiti, M., Bauzá, A., Frontera, A., Garribba, E., Gomez-García, C. J. (2019). Synthesis, structure, physicochemical characterization, and theoretical evaluation of non-covalent interaction energy of a polymeric copper(II)-hydrazone complex. Inorganica Chimica Acta, 484, 95–103. https://doi.org/10.1016/j.ica.2018.09.031

[52]. Wani, M. Y., Bhat, A. R., Azam, A., Athar, F. (2013). Nitroimidazolyl hydrazones are better amoebicides than their cyclized 1,3,4-oxadiazoline analogues: In vitro studies and Lipophilic efficiency analysis. European Journal of Medicinal Chemistry, 64, 190–199. https://doi.org/10.1016/j.ejmech.2013.03.034

[53]. Geary, W. J. (1971). The use of conductivity measurements in organic solvents for the characterization of coordination compounds. Coordination Chemistry Reviews, 7(1), 81–122. https://doi.org/10.1016/S0010-8545(00)80009-0

[54]. Siji, V. L., Sudarsanakumar, M. R., Suma, S. (2010). Synthesis and spectral characterization of zinc(II) and cadmium(II) complexes of acetone-N(4)-phenylsemicarbazone: Crystal structures of acetone-N(4)-phenylsemicarbazone and a cadmium(II) complex. Polyhedron, 29(9), 2035–2040. https://doi.org/10.1016/j.poly.2010.03.011

[55]. Belaid, S., Landreau, A., Djebbar, S., Benali-Baitich, O., Bouet, G., Bouchara, J.-P. (2008). Synthesis, characterization, and antifungal activity of a series of manganese(II) and copper(II) complexes with ligands derived from reduced N,N′-o-phenylenebis(salicylideneimine). Journal of Inorganic Biochemistry, 102(1), 63–69. https://doi.org/10.1016/j.jinorgbio.2007.07.001

[56]. Biswas, S., Mitra, K., Schwalbe, C. H., Lucas, C. R., Chattopadhyay, S. K., Adhikary, B. (2005). Synthesis and characterization of some Mn(II) and Mn(III) complexes of N,N′-o-phenylenebis(salicylideneimine)(LH_2) and N,N′-o-phenylenebis(5-bromosalicylideneimine)($L'H_2$). Crystal structures of [Mn(L)(H_2O)(ClO_4)], [Mn(L)(NCS)] and an infinite linear chain of [Mn(L)(OAc)]. Inorganica Chimica Acta, 358(8), 2473–2481. https://doi.org/10.1016/j.ica.2005.01.026

[57]. Seck, T. M., Ndoye, C., Traoré, B., Diouf, O., Thiam, I. E., Gaye, P. A., Gaye, M. (2023). Synthesis spectrospic characterization and X-ray crystal structure of heptacoordined Mn(II) complex derived from N,N'- 1,5-bis (pyridylmethylidene)carbonohydrazone ligand. IOSR Journal of Applied Chemistry (IOSR-JAC), 16, 15–22. https://doi.org/10.9790/5736-1604011522

[58]. Kose, M., Goring, P., Lucas, P., Mckee, V. (2015). Mono-, di- and tri-nuclear manganese(II) complexes derived from a quinquedentate ligand: Superoxide dismutase and catalase mimetic studies. Inorganica Chimica Acta, 435, 232–238. https://doi.org/10.1016/j.ica.2015.07.010

[59]. Sarr, M., Diop, M., Thiam, E. I., Barry, A. H., Gaye, M., Retailleau, P. (2018). Crystal structure of aquachlorido(nitrato-κ^2O,O')[1-(pyridin-2-yl-κN)-2-(pyridin-2-ylmethylidene-κN)hydrazine-κN^2]manganase(II). Acta Crystallographica Section E, 74(4), 450–453. https://doi.org/10.1107/S2056989018003493